

Thermal regime of a moraine-dammed glacial lake, Tsho Rolpa, in Rolwaling Himal, Nepal Himalayas

Akiko SAKAI¹, Tomomi YAMADA² and Kazuhisa CHIKITA³

¹ Institute for Hydropheric-Atmospheric Sciences, Nagoya University, Nagoya 464-8601 Japan

² Institute of Low Temperature Science, Hokkaido University, Sapporo 060-0819 Japan

³ Division of Earth and Planetary Sciences, Graduate School of Science, Hokkaido University, Sapporo 060-0810 Japan

(Received July 31, 2000; Revised manuscript received December 1, 2000)

Abstract

In the Nepal Himalayas there are many glacial lakes of the 1 km order scale on the surface of debris-covered glaciers. Tsho Rolpa Glacial Lake in eastern Nepal was once a small pond probably in the early 1950s, and now has become the largest glacial lake in the Nepal Himalayas. It is significant to clarify the heat source for the expansion process of a glacial lake. However, the present thermal regime of the glacial lake is still unknown. Hence, the heat balance of the lake was examined from the meteorological and hydrological data in 1993 to 1996. The result shows the increasing heat storage period of the lake was concentrated in May i.e., between the end of the ice-covered period and the start of the glacier melt season. During the monsoon season the heat loss by discharge was large, and the heat storage of the lake continue to decrease until October. During the ice-covered period from November to end of April, there are no heat input to the lake surface and no heat loss with discharge. On the other hand, the bottom ice continues to melt through a year by the heat storage in the lake.

1. Introduction

There are many glacial lakes which were glacier-dammed or moraine-dammed in Iceland, Norway, Alaska, Peru, New Zealand, China and several other countries (Thorarinson, 1939, 1957; Post and Mayo, 1971; Liestol, 1956; Lliboutry, 1977; Lliboutry *et al.* 1977a, 1977b; Kirkbride, 1993; Chen *et al.*, 1999). Such glacial lakes sometimes produced the so-called Glacial Lake Outburst Flood (GLOF) due to the moraine collapse. GLOFs of moraine-dammed lakes accompanied with huge mud flow have caused serious damage.

In the Himalayas large valley glaciers several kilometers in length have mostly debris-covered ablation areas, and occupy more than half of the glaciated areas (Moribayashi, 1974). Debris-covered glaciers advanced during the Little Ice Age between the 16th and 19th centuries. At present some debris-covered glaciers are retreating in association with the horizontal expansion of the glacial lakes which emerged during recent decades. Some debris-covered glaciers have supraglacial lakes on the termini, which are surrounded and dammed by the moraine formed during the Little Ice Age. Lake water overtopping a moraine carries sufficient energy to break easily through a moraine-dam. The overtopping of lake water is caused by a large wave, which is generated by the huge mass falling down into the lake, such as a snow or glacier avalanche from a steep slope beside the lake and also the advancing, sliding and calving of the mother glacier into the lake. Earthquakes should also be considered as an external trigger contributing to a lake-burst. GLOFs have occurred at least 13 times since the 1960s in the Arun and Sun river basins; they are the most serious natural disasters for the development of water resources (LIGG / WECS / NEA, 1988).

Kirkbride (1993) indicated that the retreating activity of a glacier terminus changes from melting to calving and that

the change accelerates the expansion of a glacial lake. Heat balance study at a glacial lake is significant to clarify the heat source of glacier ice melt which corresponds to the expansion of a glacial lake. Therefore, the purpose of this paper is to examine the present thermal regime of Tsho Rolpa, the largest glacial lake in the Nepal Himalaya.

2. Background of Tsho Rolpa Glacial Lake

In order to estimate the thermal conditions of the lake expansion at present, meteorological and hydrological observations were carried out in 1993–1996 in Tsho Rolpa Lake (27°51'N, 86°29'E), Rolwaling Valley, eastern Nepal (Fig. 1; modified Schneider's topographic map (Schneider, 1981)). The drainage area including the lake surface is 77.6 km² with the 71.8% glacial coverage; 55.3% and 16.5% are occupied by a debris-free and a debris-covered glacier (Trambau Glacier), respectively (Yamada, 1996). The lake surface area and the volume were 1.39 km² and 76.6 million m³ in 1994, respectively (Kadota, 1994).

The horizontal expansion history of Tsho Rolpa Glacial Lake has been analyzed from the data of aerial photos, topographic maps and satellite images (Earth Resources Technology Satellite [Multispectral Scanner System; MSS], MOS 1 [Multispectral Electronic Self-Scanning Radiometer] and LANDSAT [MSS]) (Mool, 1995). In 1958 the surface area was 0.23 km² according to the topographic survey by the Survey of India. Assuming that the growth rate is constant, the lake appeared probably as a pond in the early 1950s.

Chikita *et al.* (1997, 1999) have analyzed the dynamics in the lake and concluded that the surface water flow caused by the valley wind enhances ice calving at the terminus of the glacier. Sakai *et al.* (2000) estimated the expansion rate of Tsho Rolpa Glacial lake by the heat balance method. From

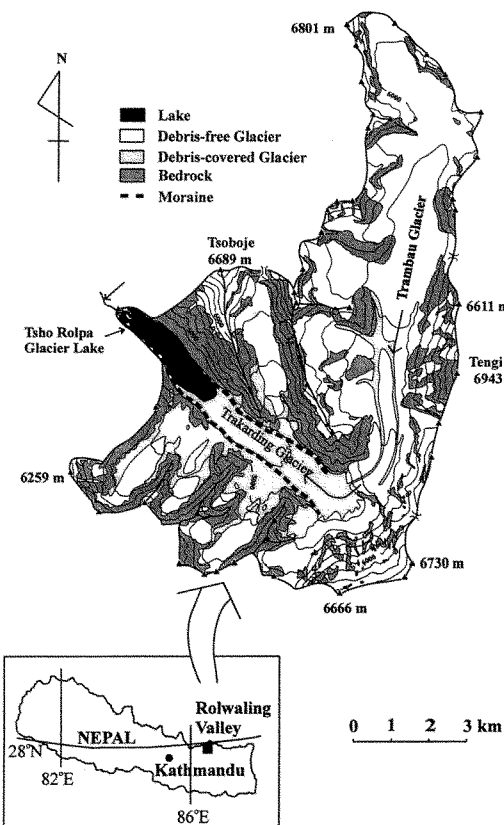


Fig. 1. Drainage basin of Tsho Rolpa Glacial Lake, Rolwaling Valley and its location in Nepal.

that calculation the present expansion rate of this glacial lake is $2.4 \times 10^6 \text{ m}^3 \text{ yr}^{-1}$, which corresponds to 3% of its present volume (76.6 million m^3).

3. Observation methods

Figure 2 shows the observation sites on the bathymetric map made in 1994 by Kadota (1994). The maximum depth is 131 m at site LD. The meteorological elements were measured at site LM on the islet 2.1 m above ground at hourly intervals from 1 June 1994 to 31 May 1995.

Surface water temperature of the lake (T_s) was also measured every hour at site LS using a thermistor sensor fixed at a water depth of about 5 cm from 8 June to 9 November 1994 during the lake surface water opening. Water level and temperature at the outlet were observed at one-hour intervals at site LO. The water level is converted to the amount of discharge by using the stage-discharge curve ($r=0.99$), which was obtained by discharge measurements in various water levels at site LO. All measured meteorological and hydrological data with accuracies are presented in Table 1 with averaged or summed data.

Vertical water temperature distributions were obtained using a water temperature depth sensor at site LV near the deepest point 8 times from 1993 to 1995. Other vertical water temperature distributions were also observed at several points along longitudinal cross section of the lake. The accuracy of depth is $\pm 0.5 \text{ m}$ and that of temperature is $\pm 0.05^\circ\text{C}$.

4. Observation results

4.1. Physical conditions of the lake

Seasonal fluctuations in water temperature were observed at site LV (Fig. 2). The water temperature fluctuated in the surface layer of less than 50 m in depth (Yamada, 1998). Below this depth, the temperature remains almost constant at about 2.7°C , in spite of the maximum density of pure water at around 4°C . This is because the suspended sediment concentration (SSC) of Tsho Rolpa is extremely high (more than 100 mg l^{-1} at the surface, more than 300 mg l^{-1} at the bottom). The bulk density is fully controlled by the amount of suspended particles which are mainly transported into the lake by the cold and highly turbid en-glacial water (Yamada, 1998). The lake water retains very stable stratification since the SSC increases almost linearly with depth throughout the year (Yamada, 1998).

The lake began to be covered with ice on 10 November 1994 by visual observation. The surface ice was about 5 cm in thickness on 22 April 1995 and covered with snow, and the lake ice had completely melted on 7 May in 1995 (personal communication with Kadota, T. and Fujita, K.). Therefore, it

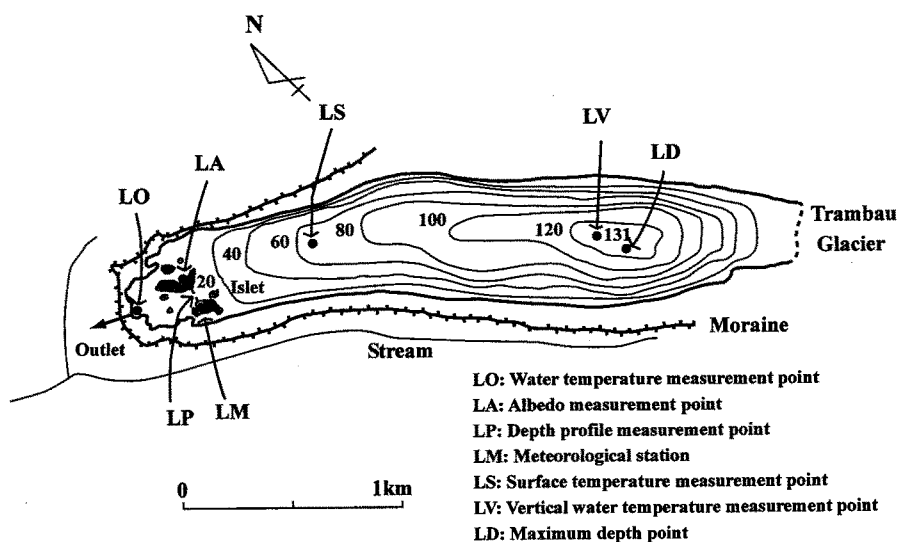


Fig. 2. Location of observation sites on the bathymetric map of Tsho Rolpa Lake. Numerical values indicate water depth in meters.

was assumed that the ice melted out on 30 April. Thus, the ice cover period was from 10 November to 30 April.

4.2. Meteorological and hydrological conditions

A time series of daily meteorological data are shown in Fig. 3 (a) and (b) from June 1994 to May 1995. Average data of the observed meteorological elements are summarized in Table 1. In the Nepal Himalaya, the rainy monsoon season begins usually in June and finishes in September. In the rainy season 1994, the solar radiation was relatively low (about 235 W m⁻² in average) and the humidity averaged 95%.

Surface water temperature of the lake (T_s) at site LS and water temperature of the outflow (T_o) at site LO through the outlet were measured every hour; the seasonal variation in the daily mean values is shown in Fig. 3(c) (Yamada, 1995). The extrapolated data of water temperature at the outlet (T_o) in 1994 were estimated from the surface water temperature T_s , and T_s in 1995 was inversely estimated from T_o as shown by a thin dashed line and a thick dashed line, respectively in Fig. 3(c), since T_s was always larger than measured T_o , which was roughly equal to ($T_s - 0.5$) in °C. Data of both T_o and T_s were not obtained from 1 to 7 June 1994, but the

Table 1. Meteorological and hydrological data from 1 June 1994 to 31 May 1995 and instrument errors. Average or total value was calculated including the interpolated data.

Elements	Average or total	Error
Air temperature	-1.1°C	0.1°C
Wind speed	2.4 m sec ⁻¹	2%
Precipitation	435 mm yr ⁻¹	0.5 mm
Relative humidity	68 %	3%
Solar radiation	219 Wm ⁻²	2 Wm ⁻²
Surface water temperature (During open water period)	5.3°C	0.4°C
Water temperature at outlet	3.5°C	0.4°C
Water level	—	3 cm
Discharge from the outlet	10.6 × 10 ⁷ m ³ yr ⁻¹	0.1 m ³ sec ⁻¹

values were assumed to be the same as the data on 8 June.

Water level data for discharge calculation were not obtained from 5 September to 15 November 1994. Discharge during the period of no water level data was estimated by the assumption that the water level decreases linearly over time in this period (-1.3 cm day⁻¹). The seasonal variation in daily discharge is shown in Fig. 3(d), where the estimated data is indicated by a dashed line. The discharge increased remark-

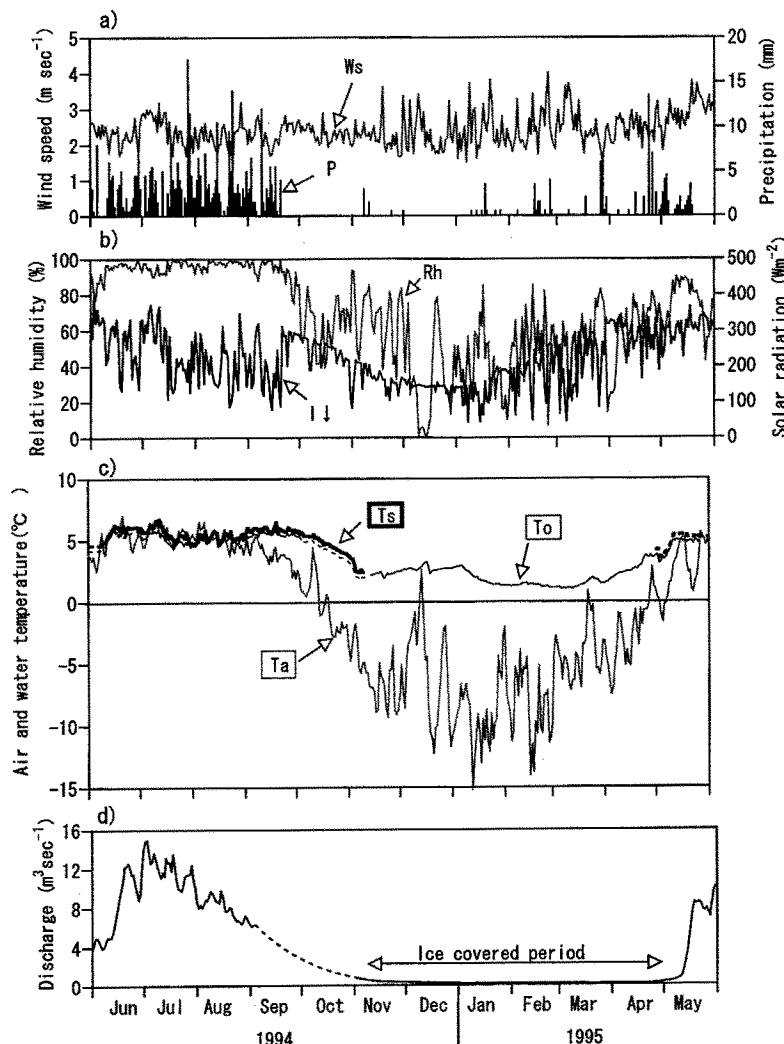


Fig. 3. Temporal variations in daily average data from 1 June 1994 to 31 May 1995 (a) wind speed, W_s , and precipitation, P ; (b) relative humidity, Rh , and solar radiation I^1 ; (c) air temperature, T_a , water temperatures, T_s at the lake surface and T_o at the outlet. Dashed lines indicate estimated values and (d) water discharge at the outlet. A dashed line indicates interpolated values.

ably in early June 1994 and reached its peak in early July 1994; thereafter it decreased gradually until early November. On the other hand, in 1995 the discharge increased in early May. The beginning of the glacier melt season varies from year to year.

5. Heat balance of the lake

5.1. Basic equation

The change in heat storage of a lake, dS/dt , consists of the net heat input at the water surface, Q_s , the heat released by water discharge at the outlet, Q_o , the heat input by meltwater inflow into lake, Q_i , and the latent heat of fusion, Q_m , for ice-melt on or below the bottom (Fig. 4). The heat balance equation is as follows.

$$\frac{dS}{dt} = Q_s + Q_i + Q_o + Q_m. \quad (1)$$

Heat input to the lake is taken to be plus, and heat outgoing from the lake is taken to be minus.

5.2. Calculation of each term

5.2.1. Change of heat storage in the lake, dS/dt

The change of stored heat in the lake, dS/dt , during the times t_1 to t_2 ($t_2 > t_1$) is defined:

$$\frac{dS}{dt} = S_2 - S_1. \quad (2)$$

The melting point of ice (273.14 K) is taken as the reference for heat content, and hence water at the melting point is regarded here as containing no heat. The average horizontal difference of vertical water temperature distribution observed at several points along the longitudinal cross section at the same time was only 0.2°C. Then, S_i ($i=1,2$) is heat storage at the time t_i . S_i is estimated by the following equation, assuming that water temperature at a certain depth is the same over the lake:

$$S_i = c\rho \int_{0}^{z_i} A(z)[T_i(z) - T_w]dz, \quad (3)$$

where c = Specific heat of water [$= 4.2 \times 10^3 \text{ J K}^{-1} \text{ kg}^{-1}$],

ρ = Density of water [$= 1000 \text{ kg m}^{-3}$],

z_i = Total depth (m) at the time t_i ,

$$T_i(z) = \text{Water temperature (K) at } z \text{ m in depth at the time } t_i,$$

$$T_w = \text{Temperature of ice melting point (=273.14 K)}$$

$$\text{and}$$

$$A(z) = \text{Area of horizontal cross section (m}^2\text{) at } z \text{ m in depth.}$$

Using the vertical temperature profiles at site LV, heat storage in the lake in various seasons was calculated as shown in Fig. 5. Although the observation frequency was limited, the heat storage tended to increase between February and May in 1994. Despite the relatively high air temperature during the summer monsoon season, the heat storage decreased with time in 1993 and also 1994.

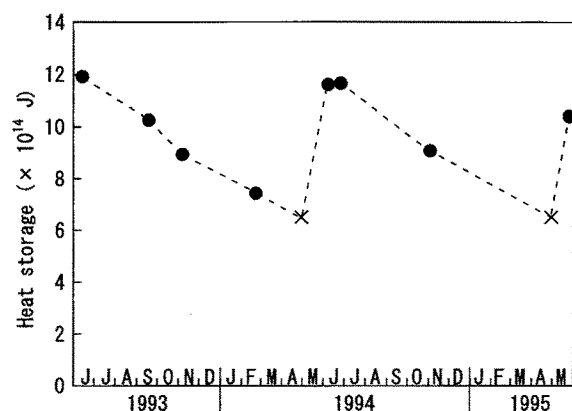


Fig. 5. Fluctuation of heat storage from 1993 to 1995. Solid circle: calculated from observed water temperature distribution. Cross: estimated for the end of ice-covered period (on 30 April, the same date in 1994 as the observation in 1995) by assuming the constant decreasing rate of heat storage during the ice-covered period and the same heat storage at the both ends.

5.2.2. Heat input, Q_s

-Open-water period-

The heat Q_s coming into the lake during the observation period (t) can be calculated by the following heat balance equation at the lake surface:

$$Q_s = \sum (I + R + H + E + P), \quad (4)$$

where I = Net shortwave radiation,

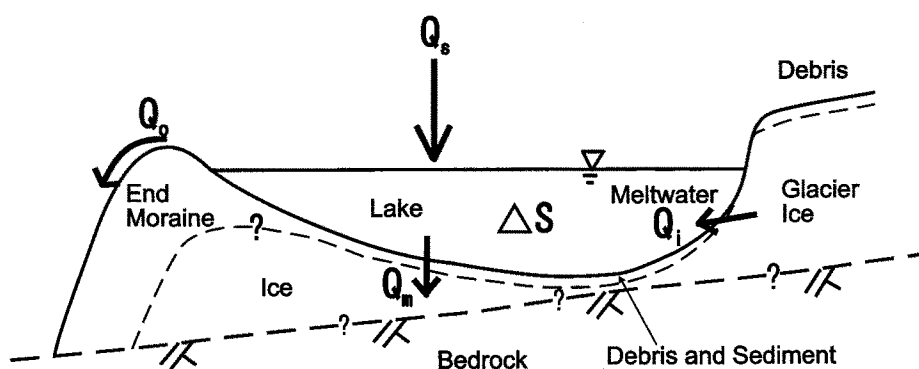


Fig. 4. Schematic image of the heat balance elements at the glacial lake. ΔS : Change of the heat storage; Q_s : heat input to the lake surface; Q_o : released heat with discharge; Q_i : heat input with meltwater; Q_m : heat loss for calving ice melt and ice melt at the bottom of the lake.

R = Net longwave radiation,
 H = Sensible heat flux,
 E = Latent heat flux, and
 P = Heat input with precipitation.

All fluxes are positive as they direct towards the lake surface.

The net shortwave radiation input to the lake surface is calculated by:

$$I = (1 - \alpha) I^{\downarrow} \quad (5)$$

The relationship between one-hour averaged albedo (α) and solar altitude (h) (in degree), obtained by Sakai et al. (2000) may be expressed as follows:

$$\alpha = 0.78 h^{-0.45}. \quad (6)$$

The albedo decreases with increasing solar altitude as shown by the power function.

Net longwave radiation input to the lake surface is expressed as:

$$R = R^{\downarrow} - \sigma T_s^4, \quad (7)$$

where R^{\downarrow} = Downward longwave radiation (W m^{-2}),
 σ = Stefan-Boltzmann constant [$= 5.67 \times 10^{-8} \text{ W m}^{-2} \text{ K}^{-4}$] and

T_s = Water temperature of the lake surface (K).

Daily mean values of the downward longwave radiation R^{\downarrow} are evaluated by the following equations (Kondo et al., 1991):

$$R^{\downarrow} = \sigma T_a^4 \left[1 - \left(1 - \frac{R_{df}^{\downarrow}}{\sigma T_a^4} \right) C \right], \quad (8)$$

$$C = 0.03B^3 - 0.30B^2 + 1.25B - 0.04, \quad B \geq 0.0323 \quad (9)$$

$$= 0, \quad B \geq 0.0323$$

with $B \equiv I^{\downarrow}/I_c^{\downarrow}$,

where T_a = Air temperature [K],

R_{df}^{\downarrow} = Global long wave radiation on clear day,

I^{\downarrow} = Global solar radiation and

I_c^{\downarrow} = Global solar radiation on clear day.

The influence of cloud for R^{\downarrow} is evaluated by the empirical equation derived on the basis of the ratio of global shortwave radiation observed to that theoretically calculated on clear days.

Sensible and latent heat fluxes were calculated by the following bulk aerodynamic formulas presented by Kondo (1975) that are applied to the wide water surface in neutral equilibrium air conditions. The bulk heat transfer coefficient for the wide water surface is here adopted because of the large fetch of the lake ($\approx 3 \text{ km}$).

$$H = c_p \rho_a C_H U (T_a - T_s), \quad (10)$$

$$E = l \rho_a C_E U (q_a - q_s), \quad (11)$$

where c_p = Specific heat at constant volume [$= 1006 \text{ J kg}^{-1} \text{ K}^{-1}$],

ρ_a = Air density [$= 0.7542 \text{ kg m}^{-3}$ at 4000 m a.s.l.],

C_H = Bulk sensible heat transfer coefficient [$= 1.80 \times 10^{-3}$],

C_E = Bulk latent heat transfer coefficient [$= 1.84 \times 10^{-3}$],

U = Wind velocity at 2 m height (m s^{-1}),

l = Latent heat for evaporation from water surface [$= 2.45 \times 10^6 \text{ J kg}^{-1}$],
 q_a = Specific humidity of air over the lake (kg kg^{-1}) and
 q_s = Specific humidity at the lake surface (kg kg^{-1}).

where q_s is for convenience assumed to be the saturated specific humidity at lake surface temperature T_s observed at site LS (Fig. 2).

Heat input with precipitation during the open-water period, P , is expressed as follows assuming that the temperature of the rain water is equal to the air temperature,

$$P = \sum c \rho (T_a - T_w) r, \quad (12)$$

where r = amount of precipitation (mm).

P was relatively small (average 0.4 W m^{-2} during open water period), since the precipitation amount was only 366 mm and air temperature was low (about 3.3°C) during the open water period. Thus, the heat input with precipitation can be neglected in this heat balance calculation.

The calculated seasonal variations of I , R , H and E during the open water period are all shown in Fig. 6(a). It is clear that the heat balance at the lake surface is mainly controlled by shortwave radiation in spite of many rainy days during the monsoon season from mid-June to the end of September. Variations of latent and sensible heat fluxes are controlled by the difference of T_a and T_s , since wind speed was almost constant (Fig. 3a) and not so strong (Table 1) all through the year. Therefore, those heat flux were nearly equal to zero from June to the end of August, and then became negative because of $T_a \cong T_s$ in the former period and $T_a < T_s$ in the latter period (Fig. 3c). The longwave radiation was negative throughout the observed period.

The seasonal variation of Q_s calculated by Equation (4) is shown in Fig. 6(b) with that of Q_o which will be discussed later. The amount of Q_s is of roughly the same order as Q_o in the monsoon season. The large variation of Q_s comes from the large variation of solar radiation. The positive value of Q_s is continuous in the monsoon season from mid-June, the beginning of the observation period, to early October. Thereafter Q_s decreases quickly, corresponding to the decreasing temperature and solar radiation as seen in Fig. 3(a) and (b).

-Ice-covered period-

Incoming heat to the lake water, Q_s , during the ice covered period can be negligible (Patterson and Hamblin, 1988) because the lake water is insulated by ice and snow layers. Therefore Q_s is assumed to be zero during the ice covered period. It was assumed that all incoming heat to the ice surface was used to melt ice during the ice melting season, because the lake surface was covered with snow just before open water on 22 April (according to personal communication with Kadota, T.), and the solar radiation could not penetrate the lake water.

5.2.3. Heat input by meltwater inflow, Q_i

The water temperature of inflowing meltwater, T_i , is probably 0°C , since it is supplied from a subaqueous tunnel mouth through en-glacial tunnels (Yamada, 1995). Hence $Q_i = c \rho q_i (T_i - T_w) = 0$, where c is specific heat of water ($= 4.2 \times 10^3 \text{ J K}^{-1} \text{ kg}^{-1}$), ρ is water density ($= 1000 \text{ kg m}^{-3}$), and q_i is meltwater inflow ($\text{m}^3 \text{ s}^{-1}$).

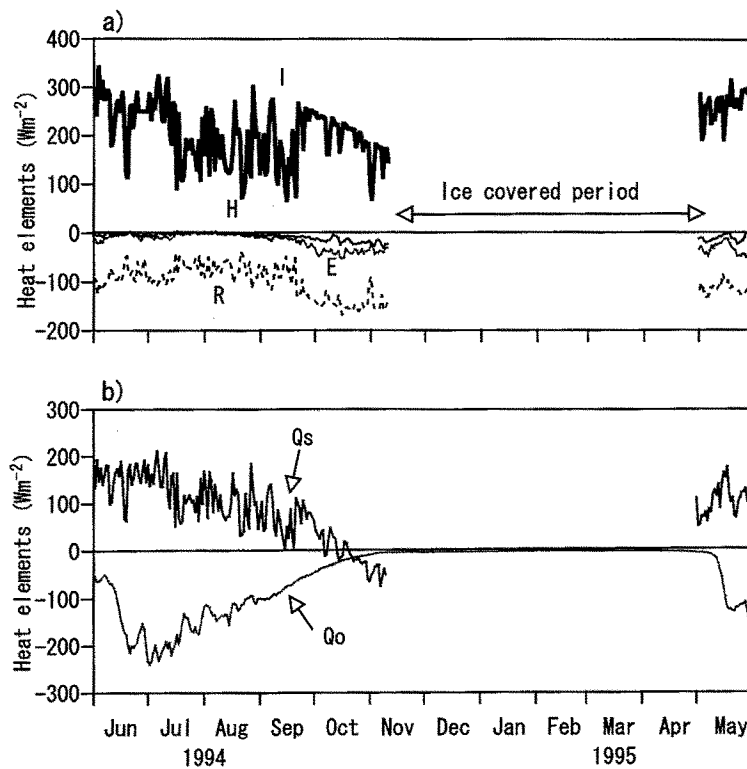


Fig. 6. Temporal variations in (a) calculated sensible heat, H ; latent heat, E ; net shortwave radiation, I ; and net longwave radiation, R ; and (b) calculated heat input to the lake surface, Q_s ; and released heat with discharge, Q_o .

5.2.4. Heat released from outflow, Q_o

Heat released from the outflow through the outlet (Q_o) is simply calculated by the following equation:

$$Q_o = \sum^t c\rho(T_o - T_w)D, \quad (13)$$

where D = Discharge amount ($m^3 sec^{-1}$) of outflow and T_o = Water temperature of outflow (K).

Fig. 6(b) shows the fluctuation of the heat, Q_o . The heat loss by discharge of the surface water increased rapidly in June with increasing discharge at the outlet and then reached its peak at the beginning of July. Thereafter it decreased gradually until November. Q_o in the ice-covered season was almost zero because discharge (average: $0.2 m^3 sec^{-1}$) and water temperature (average: $2.1^\circ C$) were comparatively low during the ice-covered period.

5.2.5. Heat loss by ice melt, Q_m

According to our observation, a cliff-shaped glacier terminus retreats by calving, and the glacier ice frequently falls into the lake only in summer. Calving produces many small icebergs in front of the glacier terminus. The icebergs floating on the lake are mostly melted by lake water. As illustrated in Fig. 4, the lake is expanded by the melting of the glacier terminus and the dead ice beneath the lake bottom. Q_m should thus be consumed by the two ways of ice melting. Sakai *et al.* (2000) evaluated the heat loss by the ice melt, Q_m , as a residual value from Eq. (1). During the ice-covered period, the heat loss at the lake bottom corresponds to the change in storage heat of about $12 Wm^{-2}$ by assuming that the heat input to the lake surface, Q_s , and released heat with outflow, Q_o , are both zero. The bottom ice of the lake was constantly melted by heat conduction in the debris

-sediment-water medium below the bottom. The melt rate of the bottom ice was thus considered to be constant, assuming no bottom sedimentation, because the water temperature at the lake bottom was almost constant throughout the year. Therefore, total heat loss for ice melt during the summer was induced to be $25 Wm^{-2}$ by adding the heat for calving ice melt ($13 Wm^{-2}$) that was observed. Consequently, Q_m was $12 Wm^{-2}$ during the ice-covered period and $25 Wm^{-2}$ during the open water period including the heat for calving ice melt.

5.3. Thermal regime of the lake

Monthly averages of the heat balance elements in a year are shown in Fig. 7. The meteorological and hydrological data of January to May 1995 and June to December 1994 are used. It was assumed that the incoming heat to the lake water was zero during the ice covered period from 10 November to 30 April. The change in heat storage is estimated as residual by Eq. (1) from monthly data because there are no monthly data on water temperature distribution.

In the beginning of May just after the disappearance of lake ice, the lake may start to absorb heat. The heat source warming the lake water up is mainly solar radiation. The other heat balance terms at the lake surface may be negligibly small because they are probably comparable to those in the summer season as shown in Fig. 6(a). Heat storage in the lake thus increases at a high rate only from May to early June. This thermal condition ceases when glacier-ice melting begins in the drainage basin. When the active glacier melting season occurs after mid-June, a large water mass with the temperature at the melting point ($0^\circ C$) comes into the lake. Meanwhile, a large warmed water mass drains out through the outlet and releases heat from the lake. Both these thermal conditions cool the lake water, and heat stor-

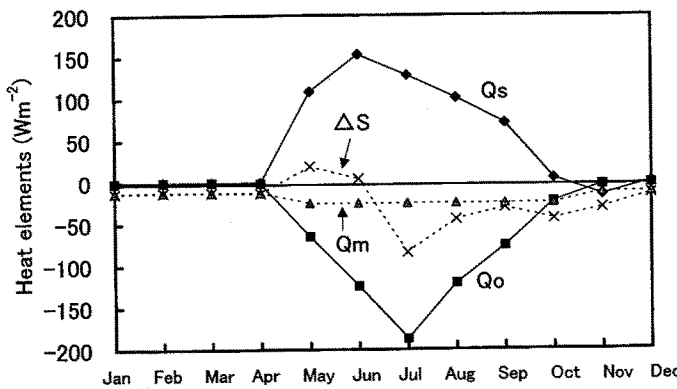


Fig. 7. Seasonal fluctuation of heat balance at the glacial lake. Monthly average heat elements estimated from the data of June 1994 to May 1995 are plotted. (Q_s : heat input to the lake surface; Q_o : released heat with discharge; Q_m : latent heat for calving ice melt and ice melt at the bottom of the lake; and ΔS : change of heat storage in the lake). Heat inflow with meltwater, Q_i is assumed to be zero all through the year because the water temperature of the meltwater inflow from the glacier must be 0°C and here, the melting point of ice (0°C) is taken as the reference for heat content. ΔS is calculated as a residual value from Eq.(1).

age in the lake decreases. This situation starts in mid-June and continues to the end of October.

The lake starts to release heat from the surface at the end of October, but the heat releasing period continues only about 20 days. The heat storage in the lake is isolated by the ice and snow layer during the ice-covered period and the lake water maintains a temperature higher than the melting point of ice and the ice melting continues at the bottom of the lake.

In order to examine the property of the above seasonal fluctuation of each heat elements, the changes in heat storage calculated as the residual values shown in Fig. 7 are compared with those of the observed values. Cross marks in Fig. 5 show the heat storage value of $6.5 \times 10^{14} \text{ J}$ on 30 April estimated by assuming that the decreasing rate of heat storage during the ice-covered period is constant until the ice melt-out on 30 April 1994. And the heat storage on 30 April 1995 is assumed to be equal to that on 30 April 1994.

Fig. 8 shows the seasonal fluctuations of heat storage change which are calculated from heat storage shown in Fig. 5 and the estimated value by the residual value in Fig. 7. The change in heat storage calculated by the observed water temperature is larger than that of the residual value from May to November especially in May.

There are several reasons for the above difference of the change in heat storage estimated by residual value and observed shown in Fig. 8. One is that the surface temperature is assumed to be always 0.5°C higher than that at the outlet. The water temperature at the outlet in May 1995 was 4.5°C . According to the above assumption, surface temperature should be 5°C , which is much higher than the melting point of ice. The surface water temperature at the beginning of May, when covered-ice just melt out, should be nearly 0°C and the heat input to the water surface should be larger than the residual value. Another reason is that there are large errors in the heat elements, Q_s and Q_o . Errors of the heat elements Q_s and Q_o are $\pm 15 \text{ W m}^{-2}$ (15%) and $\pm 10 \text{ W m}^{-2}$ (10%), respectively. Moreover, albedo and surface temperature for which data were obtained at one point (LA and LS in Fig. 2) should be inhomogeneous over the entire lake surface. These differences should induce the heat input to lake surface, Q_s , to additional errors.

Moreover, the glacial lake is surrounded by high Himalayan mountains, so longwave radiation reflecting from the exposed rockface of the mountains could lead to an underestimation of the result, R , calculated by empirical (Eqs. (7) and (8)). This would make the actual value of Q_s (Eq. (4)) to be higher than estimated.

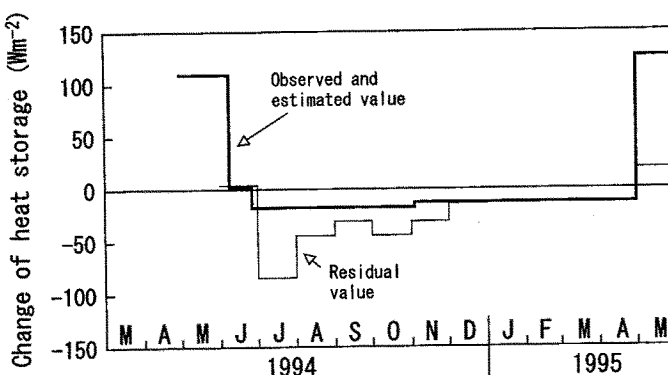


Fig. 8. Changes of heat storage calculated from heat storage in Fig. 5 (thick line) and calculated as residual value from Eq. (1) shown in Fig. 7 (thin line) from June 1994 to May 1995.

The horizontal difference in water temperature in the longitudinal direction of the lake is at most 0.6°C. Therefore, the heat storage error of the lake is $\pm 2 \times 10^{14}$ J, which corresponds to 22% of the average heat storage (9×10^{14} J). Therefore, the heat storage from the observed water temperature at LV (Fig. 2) calculated by assuming the vertical water temperature at a certain depth is the same over the entire lake is in error.

6. Concluding remarks

The heat balance all through one year in the Tsho Rolpa Glacial Lake was estimated with the hydrological and meteorological data. The thermal regime of the lake is characterized by heat absorption during the short period from late April to mid-June, i.e., from the end of the ice-covered period to the beginning of the glacier-melt season. During the glacier melt season from July to October, the heat storage in the lake has a decreasing tendency because the abundant glacier meltwater is supplied into the glacial lake, and the warmed water overflowed from the outlet. During the ice-covered period from November to April, the bottom ice continued to melt under lake water (about 3°C), which is insulated by ice from cold air (about -10°C).

In future the relation between the glacial lake expansion and the change in the thermal regime of the lake should be analyzed to clarify the process of glacial lake expansion. Furthermore, it is necessary to study the processes of bottom melting and glacier terminal calving (i.e., the interaction between lake-water and glacier ice). Specifically, the investigation of the glacier terminus and lake-bottom condition, such as the sedimentation process, is necessary.

Acknowledgments

We thank T. Kadota for his generous support and advice in the field. Our sincere thanks also to C. K. Sharma, H. M. Shrestha, and G. R. Bhatta, Executive Secretary, WECS. We are also indebted to K. P. Rizal, Officiating Executive Director, WECS, P. Mool, ICIMOD, Kiran Shankar Yogharya, and Adarsha Pokhrel, Department of Hydrology and Meteorology (DHM), who officially supported and made arrangements for our research in the field.

Financial support for our field work in Tsho Rolpa Glacial Lake was provided by JICA (Japan International Cooperation Agency), a Grant-in-Aid for Scientific Research (Project No. 06041051, No. 09490018 and Aid for JSPS Research Fellow) from the Ministry of Education, Science, Sports, and Culture of the Japanese Government, and Cooperative Research under the Japan-US Cooperative Science Program from the Japan Society for the Promotion of Science.

References

- Chen, C., Wang T., Zhang, Z. and Liu, Z. (1999): Glacial lake outburst floods in upper Nainchu river basin, Tibet. *Journal of Cold Regions Engineering*, **13**, 4, 199-212.
- Chikita, K., Jha J., and Yamada T. (1999): Hydrodynamics of a supraglacial lake and its effect on the basin expansion: Tsho Rolpa, Rolwaling Nepal Himalaya. *Arctic, Antarctic and Alpine Research*, **31**, 1, 58-70.
- Chikita, K., Yamada T., Sakai A., and Ghimire R. P. (1997): Hydrodynamic effects on the basin expansion of Tsho Rolpa Glacial lake in the Nepal Himalaya. *Bulletin of Glacier Research*, **15**, 59-69.
- Kadota, T. (1994): Report for the field investigation on the Tsho Rolpa glacier lake, Rolwaling Valley, February 1993 - June 1994. WECS Report, N551.489 KAD.
- Kirkbride, M. P. (1993): The temporal significance of transitions from melting to calving termini at glaciers in the central Southern Alps of New Zealand. *The Holocene*, **3**, 3, 232-240.
- Kondo, J. (1975): Air-sea bulk transfer coefficient in diabatic conditions. *Boundary Layer Meteorology*, **9**, 91-112.
- Kondo, J., Nakamura T., and Yamazaki T. (1991): Estimation of the solar and downward Atmospheric Radiation. *Tenki* **38**, 41-48 (in Japanese).
- Liestol, O. (1956) : Glacier dammed lakes in Norway. *Norsk Geografisk Tidsskrift* 15, **3-4**, 122-146.
- LIGG / WECS / NEA. (1988): Report on first expedition to glaciers and glacier lakes in the Pumqu (Arun) and Poiqu (Bhote-Sun Koshi) river basins, Xizang (Tibet), China. Sino-Nepalese Joint Investigation of Glacier Lake Outburst Flood in Himalayas in 1987, Lanzhou Institute of Glaciology and Geocryology, Academia Sinica, and Water and Energy Commission Secretariat of Nepal, Science Press, Beijing, 192 pp.
- Lliboutry, L. (1977): Glaciological problems set by the control of dangerous lakes in Cordillera Blanca, Peru. II. Movement of a covered glacier embedded within a rock glacier, *J. Glaciol.* **18**, **79**, 235-273.
- Lliboutry, L., Morales B., Pautre A., and Schneider B. (1977a): Glaciological problems set by the control of dangerous lakes in Cordillera Blanca, Peru. I. Historical failures of morainic dams, their causes and prevention. *J. Glaciol.* **18**, **79**, 239-254.
- Lliboutry, L., Morales B., and Schneider B. (1977b): Glaciological problems set by the control of dangerous lakes in Cordillera Blanca, Peru. III. Study of moraines and mass balances at Safuna. *J. Glaciol.* **18**, **79**, 275-290.
- Moribayashi, S. (1974): On the characteristics of Nepal Himalayan glaciers and their recent variations. *Seopyo* **36**, 11-21.
- Mool, K. P. (1995) : Glacier lake outburst floods in Nepal. *J. Nepal Geological Society*, Kathmandu, 11, Special Issue: 273-280.
- Patterson, J. C. and Hamblin P. F. (1988): Thermal simulation of a lake with ice cover. *Limnology & Oceanography*, **33**(3), 323-338.
- Post, A. and Mayo L. R. (1971): Glacier dammed lakes and outburst floods in Alaska. *Hydrological Investigations Atlas HA-455*, U.S. Geological Survey, Department of the Interior, Washington, D. C., 10 p. +3 maps.
- Sakai, A., Chikita K. and Yamada T. (2000): Expansion of a moraine-dammed glacial lake, Tsho Rolpa, in Rolwaling Himal, Nepal Himalaya. *Limnology & Oceanography*, **45**, 1401-1408.
- Schneider, E. (1981): Topographic map of Rolwaling Himal, Nepal -Kartenwerk der Arbeitsgemeinschaft für vergleichende Hochgebirgsforschung Nr.4, Research scheme Nepal Himalaya.
- Thorarinsson, S. (1939): The ice dammed lakes of Iceland with particular reference to their values as indicators of glacier oscillations. *Geografiska Annaler*, Årg. 21, Ht. 3-4, 216-242.
- Thorarinsson, S. (1957): The jökulhlaup from the Katla area in 1955 compared with other jökulhlaups in Iceland. *Jökull. Ár.* **7**, 21-25.
- Yamada, T. (1995): Data report on meteorological and hydrological data at Tsho Rolpa Glacier Lake, Rolwaling Himal - from June 1993 to May 1995 -. WECS Report N551.498 DAT.
- Yamada, T. (1996) : Report of the investigations of Tsho Rolpa Glacier Lake, Rolwaling Valley, WECS / JICA, 35pp.
- Yamada, T. (1998) : Glacier lake and its outburst flood in the Nepal Himalaya, Monograph No. 1, Data Center for Glacier Research, Japanese Society of Snow and Ice. 96 pp.

LIGG: Lanzhou Institute of Glaciology and Geocryology

WECS: Water and Energy Commission Secretariat

NEA: Nepal Electricity Authority

JICA: Japan International Cooperation Agency